

RADIATION CHEMISTRY

PREPARATION AND PROPERTIES OF PROPYLENE OXIDE FLUOROPOLYMERS

I. P. Kim, A. F. Shestakov, Yu. M. Shulga, V. Y. Gak, S. R. Allayarov

Federal State Budgetary Institution of Science Federal Research Center for Problems of Chemical Physics and Medicinal Chemistry of the Russian Academy of Sciences, ave. akad. Semenova, 1, Chernogolovka, Moscow region, 142432 Russia

E-mail: ipkim@icp.ac.ru

Received July 11, 2024

Revised July 11, 2024

Accepted September 05, 2024

In solutions of tetrafluoroethylene in propylene oxide with concentrations of 0.08–4.2 mol/l, telomeres are formed under the action of gamma rays from a ^{60}Co source at room temperature, the chain length of which depends on the monomer content in the solution. The monomer consumption during irradiation was controlled calorimetrically and gravimetrically, and its complete conversion was observed at radiation doses of 10–15 kGy. The molecular mass characteristics of the radiolysis products were determined by thermogravimetry. Telomeres with a chain length of less than 6 form true solutions. When the degree of polymerization of the monomer is 6–15, colloidal solutions are formed, and when it is more than 15, dense gels are formed. The structure of the fluorotelomer of propylene oxide retains the terminal functional epoxy group. The morphology of the coating layers was studied by atomic force microscopy.

Keywords: radiation telomerization, tetrafluoroethylene, propylene oxides, fluorotelomer, hydrophobicity, quantum chemical modeling, AFM, ICS

DOI: 10.31857/S00231193250108e9

INTRODUCTION

Perfluorinated (PF) oligomers are promising for obtaining new useful materials and precursors: polymer membranes for fuel cells [1], low-loss polymer optical fibers [2, 3], thermo- and corrosion-resistant and ultrahydrophobic thin-layer coatings [4, 5]. This is due to the uniquely high strength, rigidity, and weak intermolecular interaction of PF carbon chains. In order to realize these possibilities, it is necessary, in particular, to find the conditions under which oligomers with a chain

length optimal for a given application are formed. Currently, such studies are widely conducted abroad [5-15]. The main difficulty of such studies is related to the fact that PF oligomers with a chain length greater than 4-6 monomeric units form not homogeneous, but colloidal solutions that turn into gels with increasing concentration of oligomers and chain length. Phase transitions, in turn, affect the polymerization process by changing the ratio of growth rate constants and chain transfer.

The production of oligomers with end groups capable of further polymerization opens up possibilities for designing polymers with special architecture (flexible main chain with variable link length and side chains of rigid perfluorinated rods of various lengths). Polymers with "brush" or "comb" architecture (flexible main chain with attached oligomeric side groups [5-8]) are obtained by polymerization of monomers forming the main chain, to which side groups of different lengths are preliminarily attached. For example, acrylates and methacrylates are used as the main chain, and soluble perfluorinated alcohols with chain lengths from 1 to 4 tetrafluoroethylene units (**TFE**) are used as side groups [8, 9]. The production of polymers with longer PF side chains and varying main chain link lengths has not been described, although these parameters determine the properties of "brushes." Moreover, increasing the length of PF side groups is interesting because it will lead to a decrease in the volume fraction of CH groups, and thereby reduce losses in optical fiber. During the polymerization of TFE in a cyclic ether – tetrahydrofuran (**THF**) – the structure of the solvent end groups is preserved, i.e., reactive monomers for the synthesis of branched polymers are formed [5]. The polymerization of THF and its derivatives is described in [10, 11].

Ultra-hydrophobicity is achieved by combining the hydrophobicity of the coating material with its nanoscale roughness. In particular, nanoscale structures are formed from amphiphilic aggregates, which simultaneously include hydrophobic and hydrophilic groups [12, 13]. Self-organization of molecules into supramolecular structures, caused by bonds between functional groups with a given arrangement, is considered as one of the main methods for obtaining nanostructured materials [14]. The role of functional groups is played by substituents capable of forming intermolecular hydrogen and coordination bonds [15].

By changing the nature of the solvent and the concentration of the monomer during radical telomerization of TFE, it is possible to vary the chain length and composition of the end groups. The purpose of this work – is to study the properties of radiation telomerization products of TFE in propylene oxide solutions

EXPERIMENTAL PART

A cyclic ether – propylene oxide ($\text{CH}_2\text{CHOCH}_3$) (**PO**) (from Acros, 99% purity), containing an epoxy group, was selected as the solvent (telogen). Telomers were obtained according to the method [16,17] by irradiating TFE solutions of various concentrations (0.2 – 4.2 mol/L) in the solvent in sealed glass ampoules. Radiolysis was carried out on the UNU "Gammatok-100" gamma unit of the FRC IPCP and MS RAS at room temperature with an integral dose of 10–15 kGy, at which complete conversion of TFE occurs.

Solvents were preliminarily degassed on a vacuum unit to a residual pressure of 1.333 Pa at -196°C , then the required amount of TFE was frozen into the ampoule and sealed. Analysis of the reagent mixture was carried out using a differential scanning calorimeter (**DSC**) in the temperature range from -196°C to 27°C . For TFE $T_m = -142.5^\circ\text{C}$, $T_b = -76.3^\circ\text{C}$, $\text{PO} - T_m = -112^\circ\text{C}$, $T_b = 34.2^\circ\text{C}$. TFE consumption was determined calorimetrically by measuring the specific heats of fusion of the reagents and gravimetrically.

Differential thermogravimetry (**DTG**) measurements were carried out on a "Q-1500D" derivatograph in an open corundum crucible. Heating rate $5^\circ\text{C}/\text{min}$, sample weight – 50 – 100 mg, reference – Al_2O_3 . Samples were prepared by removing the solvent from the irradiated solutions by drying at room temperature or by vacuum distillation.

Quantum-chemical modeling of radical reactions leading to the formation of telomers in the TFE + OP system was performed using the PBE density functional [18] and an extended basis set: C,O,F [5 s 5 p 2 d /3 s 3 p 2 d], H[5 s 1 p /3 s 1 p] for valence electrons and SBK pseudopotential [19]. All calculations were performed using the PRIRODA software package [20] with the computational capabilities of the Joint Supercomputer Center of the Russian Academy of Sciences

IR spectra were recorded at room temperature with a resolution of 4 cm^{-1} in the range of 4000–400 cm^{-1} using a "Perkin Elmer Spectrum Two" FTIR spectrometer with an attenuated total reflection (ATR) accessory.

The morphology of coating layers was measured using an atomic force microscope (**AFM**) "Integra Aura" by NT-MDT (Zelenograd, Russia) at room temperature in amplitude and phase imaging modes.

RESEARCH RESULTS AND DISCUSSION

When freezing the binary mixture of TFE + telogen in the calorimeter block to -196°C for all studied concentrations of TFE in telogen, individual substances form their own crystalline phase, and when thawing the mixture to 27°C , two melting peaks are recorded – for the monomer and the solvent.

On the thawing curves of radiolysis products at a dose of 5 kGy in the temperature range from -196°C to 27°C , the TFE melting peak is not observed, only the solvent melting peak remains. Even at such low integral doses, TFE is almost completely involved in the telomerization reaction. Gravimetric measurements also showed that TFE is almost completely consumed during the radiolysis of TFE solutions in OP.

The homogeneity of the OP fluorotelomer depends on the initial concentration (C_0) of TFE in OP. Telomer solutions in PO remain homogeneous at $C_0 < 0.2 \text{ mol/L}$. In more concentrated solutions, opalescence appears, indicating the formation of colloidal particles, i.e., transition through the lower boundary of phase separation [16]. The appearance of a homogeneous gel (upper boundary of phase separation) is observed at $C_0 > 0.6 \text{ mol/L}$. Telomerization products of TFE with chain lengths greater than 5, as shown in [16, 17, 21], form micron-sized colloidal particles consisting of telomers solvated by the solvent.

To determine the molecular weight distribution (**MWD**) of oligomers with the number of units $n > 6$ and the total fraction of oligomers with $n > 15$, the thermogravimetric analysis method proposed in [22, 23] was used. The MWD of telomers obtained by γ -radiolysis of TFE solutions of various concentrations in PO, calculated from experimental thermogravimetry data, are shown in Fig. 1. It can be seen that with increasing concentration of TFE in the initial solution, the relative yield of high-molecular-weight telomers increases (Fig. 1, curves 1-3).

In the case of propylene oxide with $T_{\text{boil}} = 34.2^{\circ}\text{C}$, lower telomers with $n = 1-2$ have boiling points less than or about 100°C , therefore losses of these fractions are possible when drying samples for thermogravimetric measurements. The MWD curve of the sample at $C_0 = 0.6 \text{ mol/L}$ (Fig. 1, curve 1) shows that the radiolysis product consists mainly of telomers with $n = 3-5$. With increasing concentration of TFE in the irradiated mixture, the proportion of telomers with longer chain length increases - Fig. 1, curve 2 . At $C_0 = 2-4 \text{ mol/L}$, higher telomers with chain length $n > 15$ are formed, creating a dense gel, and their fraction increases to 0.9.

For the studied solvents, with increasing initial concentration of TFE in OP, phase transitions from ideal to colloidal solution and then to gel are observed. A characteristic feature of colloidal solutions is the increase in the oligomer/solvent ratio with increasing initial TFE concentration in the solution [22]. The change in the MMD shape occurs in the TFE concentration range where colloidal particles form. In colloidal solutions, the MMD becomes bimodal (Fig. 1). The low molecular weight component has a maximum at $n = 3-5$ and decreases in intensity with increasing C_0 . The maximum of the high molecular weight component appears in the C_0 range where the ideal solution transitions to colloidal and shifts with increasing C_0 toward larger n . At $C_0 \approx 0.6 \text{ mol/l}$, when a gel forms, the

mass fraction of low molecular weight oligomers ($n \leq 5$) becomes less than the fraction of oligomers with chain length $n \geq 15$. In the temperature range exceeding the degradation temperature, it is only possible to determine the fraction of oligomers with chain length $n \geq 15$.

Experimental studies of coating morphology are presented in Fig. 2. Colloidal solutions of OP fluorotelomers were poured onto the surface of substrates made of a luminum deformable alloy and dried at 23 °C for 1-2 hours, forming layers with a thickness of about 10 - 30 μm . Changes in the coating structure were made by heating for 1-2 hours at a temperature of 100 °C. With the initial removal of free solvent not included in the colloidal particles, a "loose" xerogel is formed, consisting of weakly bound conglomerates in which the structure of colloidal particles is predominantly preserved. The average height of the coating relief differences is $\sim 1.0 \mu\text{m}$ (Fig. 2a). There are no relatively flat areas between the relief differences, which apparently corresponds to tightly arranged relief protrusions (lumps) adjacent to each other. From the above, it follows that at room temperature, the coating is continuous, although it is uneven in thickness periodically along any chosen direction. In the subsequent drying process with heating at 100 °C, the average size of colloidal particles decreases from 1 to 0.5 μm due to partial removal of the solvent and oligomers with short chains included in their composition, and the associated compaction of the framework (Fig. 2b). Slow evaporation of the solvent from the gel occurs during heat treatment, accompanied by deformation of the framework and formation of an aerogel with new structural elements of micron (dense conglomerates and microfibers connecting them) and nanoscale dimensions. In work [17] and in this work, the polymerization of TFE in solutions of cyclic ethers with the formation of telomers that retain a reactive functional group suitable for subsequent polymerization [5, 10, 11] was studied. Preservation of cycles capable of further polymerization opens up an interesting possibility of obtaining copolymers with rod-coil type structures, in which perfluorinated oligomers are the rods. Polymers with such architecture, but with simpler substituents, have attracted attention recently [25, 26].

Conducting polymerization of fluorotelomers will make it possible to obtain polymers with a flexible hydrophilic main chain and rigid perfluorinated hydrophobic side chains of various lengths. The size of the main polymer unit can be varied by selecting the telogen depending on the polymerization ability of the end group, and the length of the side perfluorinated group will be determined by the degree of TFE polymerization in the telomer.

Telomerization of TFE in THF occurs with chain transfer through the α -hydrogen of the furan ring with preservation of the five-membered ether cycle, and short-chain telomers are formed even at high concentrations of TFE, which indicates a high value of the ratio of chain transfer to growth rate

constants [17]. This is confirmed by the results of quantum-chemical modeling, showing the practical absence of H atom detachment from the THF molecule during telomerization [17].

When using EP with a three-membered ether cycle as a telogen, with increasing concentration of TFE in solution, the proportion of higher telomers increases and the formation of true solutions, colloidal solutions, and gels is observed. The ratio of chain transfer to growth rate constants, as a function of its length n , found from measurements of MMD of TFE telomerization products in solvents with the formation of higher telomers, as shown in [24], increases by 1.5 – 2.5 times in the range n from 2 to 5, is almost constant in the range n from 6 to 10, and increases by 7–10 times in the range n from 12 to 20.

As a result of chain breakage by transferring an H atom from PO to a macroradical, primary, secondary, or tertiary radicals can be formed. The calculation of activation energy for corresponding model reactions using the PBE density functional gave values of 5.4, 3.3, and 2.6 kcal/mol (see the structure of transition states (a, b, c) in Fig. 3). For a similar reaction of H atom abstraction from the α -C–H bond of THF, a notably lower value of 0.7 kcal/mol was obtained, which fully corresponds to an earlier transition state, the distance $-\text{CF}_2\ldots\text{H}$ equals 1.50 Å, compared to 1.38 Å when forming a secondary radical from PO (see Fig. 3b). Possible addition processes of a macroradical to the O atom with opening of the oxetane ring are unlikely, as they require activation energies of 12.6 and 11.7 kcal/mol, respectively (see Fig. 3d, 3e). Thus, the reactivity of the methyl group is the lowest, and the most probable secondary radicals from propylene oxide are radicals with a free valence in the three-membered ring. Further addition processes of these radicals to the double bond of TFE require insignificant activation energies of 0.2, 0.1, and 2.7 kcal/mol for primary, secondary, and tertiary radicals, respectively (see the TS structure in Fig. 4).



In the system $\text{C}_2\text{F}_5\bullet + \text{C}_2\text{F}_4 + \text{CH}_3\text{F}_5 + \text{CHMe-CH}_2$, which models the reaction mixture, two radical reactions may occur: H atom abstraction from PO and addition to TFE. The calculated difference in activation energy for the abstraction of a tertiary H atom is 1.5 kcal/mol. This gives a difference in the corresponding rate constants by a factor of 15 at room temperature. Taking into account that the molar fraction of TFE is an order of magnitude less than the molar fraction of PO, this result is consistent with the short length of the resulting oligomers in experiments.

It should also be considered that the isomerization of primary radicals from OP with oxetane ring opening to form acyclic radicals $\text{Me-CO-CH}_2\bullet$, $\text{Me-CH}\bullet-\text{CHO}$ and $\text{CH}_2=\text{CH-O-CH}_2\bullet$

proceeds with an energy gain of 32.9, 34.9, and 3.3 kcal/mol, respectively (Fig. 5). The transition states for these reactions are located approximately 10 kcal/mol above the corresponding initial cyclic forms. Estimation of the isomerization rate constant under standard conditions based on activated complex theory and calculated partition functions gives a value of about 10^{-6} s⁻¹. For a typical monomer concentration of ~ 1 mol/L and the addition rate constant [21] of carbon-centered radicals from the solvent to TFE equals 2.0×10^{-9} L/mol s. As can be seen, the rate of primary radical addition to the double bond is much higher than their isomerization rate. Thus, it is unlikely that the isomeric radicals $\text{Me}-\text{CO}-\text{CH}_2\bullet$, $\text{Me}-\text{CH}\bullet-\text{CHO}$ and $\text{CH}_2=\text{CH}-\text{O}-\text{CH}_2\bullet$ could be telomer end groups. However, in this case, characteristic stretching $\text{C}=\text{O}$ and $\text{C}=\text{C}$ vibrations should appear in the IR spectrum of the product, which can be experimentally detected. According to the performed calculations for telomers $\text{CH}_3-\text{CO}-\text{CH}_2\text{C}_6\text{F}_{13}$, $\text{CH}_3-\text{CH}(\text{C}_6\text{F}_{13})-\text{CHO}$ and $\text{CH}_2=\text{CH}-\text{O}-\text{CH}_2\text{C}_6\text{F}_{13}$, the corresponding stretching vibrations of double bonds have wave numbers 1732 (11.5%), 1764 (9.9%) and 1630 (10%) cm⁻¹, where the values in parentheses are the ratio of these vibrations' intensity to the total intensity of C-F stretching vibrations of these telomers with $c n = 3$.

The most intense bands in the IR spectrum of the sample (Fig. 6) are stretching vibrations (ν) of C–F bonds (1201 and 1146 cm⁻¹) [27]. Bands in the low-frequency region of the spectrum (638, 554, and 501 cm⁻¹) are associated with wagging, deformation, and rocking vibrations of CF_2 -groups. Confirmation of the assumption that the telomer contains end groups formed as a result of the interaction between the oligomeric TFE chain and radiation degradation products of propylene oxide comes from the presence of three peaks at 2983, 2931, and 2854 cm⁻¹.

The inset of Fig. 6 shows a fragment of the spectrum in the region of $\text{C}=\text{O}$ bond stretching vibrations. We propose the following assignment of peaks in the shown fragment. Peaks at 1789 and 1727 cm⁻¹ correspond to stretching vibrations of $\text{C}=\text{O}$ bonds. The intensity of the peak at 1681 cm⁻¹ includes contributions from stretching vibrations of carbonyl groups, vibrations of $\text{C}=\text{C}$ double bonds, and deformation vibrations of water molecules. Water adsorption should be taken into account since O–H vibration peaks are present in the spectrum of the studied sample.

It can be noted that the literature provides convincing evidence that during PTFE degradation, peaks appear in the region from 1800 to 1650 cm⁻¹, which are associated with stretching vibrations of groups such as $-\text{CF}=\text{CF}_2$ (1785 cm⁻¹), $-\text{CF}=\text{CF}-$ (1730 and 1717 cm⁻¹) [28]. However, this also produces vibrations of COF (1883 cm⁻¹) and CF_3 (985 cm⁻¹) groups, which were not detected in the studied sample. Therefore, the observed peaks at 1789 and 1727 cm⁻¹ have a different nature.

To determine the relative intensities of individual peaks at the quantitative level, this part of the spectrum was converted to "absorption" mode with background subtraction based on its linear

approximation. (see Fig. 6.) The integral intensity of the group of peaks in the region of C=O bond stretching vibrations (spectral range 1842–1571 cm⁻¹) of this group of peaks is 0.83% of the integral intensity of peaks caused by C–F bond stretching vibrations (spectral range 1350–900 cm⁻¹, Fig. 6). Comparing the relative intensity with the theoretical one (see above), it can be assumed that the total yield of telomers with an opened oxetane cycle is approximately 8%.

Figure 6 and Table 1 show the description of the group of peaks in the spectral range 1842–1571 cm⁻¹ using Gaussian lines. Peak assignments were made based on literature data [29]. The results of decomposition, when all parameters were varied, showed that three peaks (2 , 4 and 5) are sufficient to describe this fragment of the spectrum. Minor peaks 1 , 3 and 6 can be considered as fitting adjustments. The main contribution to this part of the spectrum is made by the stretching vibrations of the carbonyl group. The second most important contribution we associate with the vibrations of C=C double bonds (1650 cm⁻¹, peak 5). We believe that the value of 1650 cm⁻¹ slightly exceeds the characteristic value for the deformation vibrations of adsorbed water molecules. The attempt to introduce adsorbed water (peak 6) can be considered unsuccessful. Peaks at 1650 and 1733 cm⁻¹ agree well with the calculated values of 1630 and 1732 cm⁻¹ for C=C and C=O vibrations. For the CO vibration of the terminal HCO group, the calculated value of 1764 differs most significantly from the experimental 1682 cm⁻¹. This can be associated with a stronger influence of the environment, since for a telomer with a terminal C=O group, the dipole moment is 4 D, which is 2 times greater than for isomers.

Table 1. Results of decomposition of the IR spectrum fragment (Fig. 6) and assignment of individual peaks

Peak	Position, cm ⁻¹	Half-width, cm ⁻¹	Intensity, %	assignment
1	1794	24	4.0	ν (C=O)
2	1733	74	46.3	ν (C=O)
3	1727	23	3.9	ν (C=O)
4	1682	39	19.4	ν (C=O)
5	1650	64	26.3	ν (C=C)
6	1621	6	0.1	δ (H ₂ O)

This causes a greater energy effect of interaction with the environment, and consequently its greater influence on the properties of the telomer. As an example, we can cite the rather large interaction energy of the main telomers (without opening dioxetane cycles) involving the epoxide O atom and C–H bond of the terminal CF₂H group (see Fig. 7), which is 2.8 kcal/mol and 2.1 kcal/mol at distances H–O = 2.23 and 2.28 Å, for structures (a) and (b) in Fig. 7 respectively.

Taking into account the proximity of molecular characteristics of acetone and PO as solvents, we can use the estimation of the average degree of TFE polymerization from [21]

$$\bar{n} \approx 2 * 10^{-2} C \exp(E_a / RT) \quad (1),$$

where C is the concentration of TFE in mol/l, E_a is the activation energy of chain transfer reactions to the solvent. For the calculated value of $E_a \sim 3$ kcal/mol and $C \sim 1$ mol/l, it gives a value of 4, which is in good agreement with experimental data.

CONCLUSIONS

In solutions of tetrafluoroethylene in propylene oxide with concentrations of 0.08-4.2 mol/l at low integral radiation doses (~ 10 kGy), telomers are formed, the chain length of which depends on the monomer concentration. Solutions of telomers in PO with chain length $n < 6$ remain homogeneous at an initial TFE concentration < 0.2 mol/l. In more concentrated solutions, colloidal particles with an average chain length $n = 6-15$ are formed. The appearance of a homogeneous gel is observed at an initial TFE concentration greater than 0.6 mol/l (with chain length $n > 15$). In the structure of PO fluorotelomer, the terminal functional epoxy group is mainly preserved.

FUNDING

The work was carried out according to the State Assignment FFSG-2024-0007 №124013000722-8.

REFERENCES

1. *Ivanchev S.S., Myakin S.V.* // Uspekhi Khimii. 2010. V.72. P.117.
2. *White W.R., Dueser M., Reed W.A., Onishi T.* // IEEE Photonics Techn. Lett. 2000. V.12. P.347.
3. *Gravina R., Testa G., Bernini R.* // Sensors. 2009. V.9. P.10423
4. *McKeen L.W.* / Fluorinated coatings and finishes handbook. PDL Series. Andrew Publ. N.Y. 2005.
5. *Ameduri B., Boutevin B.* / Well-architected fluoropolymers: Synthesis, properties and applications. Elsevier. Amsterdam. 2004.
6. *Potemkin I.I., Palyulin V.V.* // Polym. Sci. Ser. A. 2009. V.51. P.163.
7. *Erulkhovich I., Theodorakis P.E., Paul W., Binder K.* // J. Chem. Phys. 2011. V.134. 054906.
8. *Soules A., Pozos C., Ameduri B., Joly-Duhamel C., Essahli M., Boutevin B.* // J. Polym. Sci. A. 2008. V.46. P.3214.
9. *Schuman P.D.* / US Patent 5690863, November 25, 1997.
10. *Mah S., Choi J., Lee H., and Choi S.* // Fibers and Polymers. 2000. V.1. P.1.

11. *Chen Y., Zhang G., Zhang H.* // *J. Appl. Polym. Sci.* 2001. V.82. P.269.
12. *Casagrande C., Fabre P., Raphael E., Veyssie M.* // *Europhys. Lett.* 1989. V.9. P. 251.
13. *Dendukuri D., Hatton T.A., Doyle P.S.* // *Langmuir* 2007. V. 23. P. 4669
14. *Elemans A.A.W., Lei S., De Feyer S.* // *Angew. Chem. Int.Ed.* 2009. V. 48. P.7298.
15. *Cadeddu A., Ciesielski A., El Malah T., Hecht S., Samori P.* // *Chem.Commun.* 2011. V.47. P. 10578.
16. *Kim I. P., Shestakov A. F.* // *High Energy Chemistry.* 2009. V.44. P. 516.
17. *Kim I. P., Perepelitsina E.O., Shestakov A. F., Shulga Yu. M., Kunitsa A.A.* // *High Energy Chemistry.* 2011. V. 45. № 6. P.511.
18. *Perdew J. P., Burke K., Ernzerhof M.* // *Phys. Rev. Lett.* 1996. V.77. P.3865.
19. *Stevens W.J., Bash H., Krauss M.* // *J. Chem. Phys.* 1984. V.12. P. 6026
20. *Laikov D. N.* // *Chem. Phys. Lett.* 1997. V. 281. P.151.
21. *Shestakov A. F., Kim I.P.* // *High Energy Chemistry.* 2009 . V.44 . P. 555.
22. *Kim I. P., Kolesnikova A. M.* // *Russian Journal of Physical Chemistry .* 2011 . V. 85 . P.1782 .
23. *Kim I. P.* // *High Energy Chemistry.* 2011. V.45 . P. 399 .
24. *Kim I. P., Bendersky V. A.* // *High Energy Chemistry.* 2011 . V. 45 . P. 406 .
25. *Zhang Y., Lam Y.M.* // *J. Colloid and Interface Sci.* 2005 . V.285 . P.80.
26. *Chou S-H., Tsao H-K., Sheng Y-J.* // *J. Chem. Phys.* 2011. V. 134. P.034904
27. *Liang C. Y., Krimm S.* // *J. Chem. Phys.* 1956. V.25. P.563.
28. *Lappan U., Geißler U., Lunkwitz K.* // *Radiation Physics and Chemistry.* 2000. V.59. P. 317(2000).
29. *Smith A.L. / Applied Infrared Spectroscopy: Fundamentals, Techniques, and Analytical Problem-Solving.* John Wiley & Sons: Chichester, UK. 1979.

Figure Captions

Fig. 1. MMD curves based on thermogravimetry data of TFE telomers in OP with initial solution concentration (mol/l): 0.6 (1), 1.0 (2), 4.2 (3).

Fig. 2. AFM images of coatings based on OP fluorotelomer on the surface of wrought aluminum alloy in amplitude representation - upper panel, and relief - lower panel. Observation area $40 \times 40 \mu\text{m}$. Coating drying was carried out at 23°C (a), 100°C (b).

Fig. 3. Structure of the transition state during H atom abstraction by $\text{C}_2\text{F}_5\bullet$ radical from primary (a), secondary (b), and tertiary (c) C-H bonds of OP (a-c), as well as its addition to the O atom (d, e). Distances are indicated in Å.

Fig. 4. Structure of the transition state during the addition of primary (a), secondary (b), and tertiary (c) radicals from OP to TFE. Distances are indicated in Å.

Fig. 5. Energy diagram of isomerization and the structure of the transition state upon the addition of secondary (a), tertiary (b), and primary (c) radicals from OP. Distances are indicated in Å. Energy levels are given relative to the initial system $\text{C}_2\text{F}_5\bullet + \text{OP}$.

Fig. 6. IR spectrum after supercritical drying of the telomer sample obtained during the telomerization of TFE in OP with an initial solution concentration of 0.8 mol/l. The inset shows a fragment of the IR spectrum in the region of stretching vibrations of C=C and C=O bonds in "absorption" mode and its approximation by individual peaks.

Fig. 7. Structure of a complex of two telomers connected by a hydrogen bond at the terminal CF_2H -groups and an O atom of the OP fragment with a macroradical attached to the CH_3 -group (a) or oxetane cycle (b).

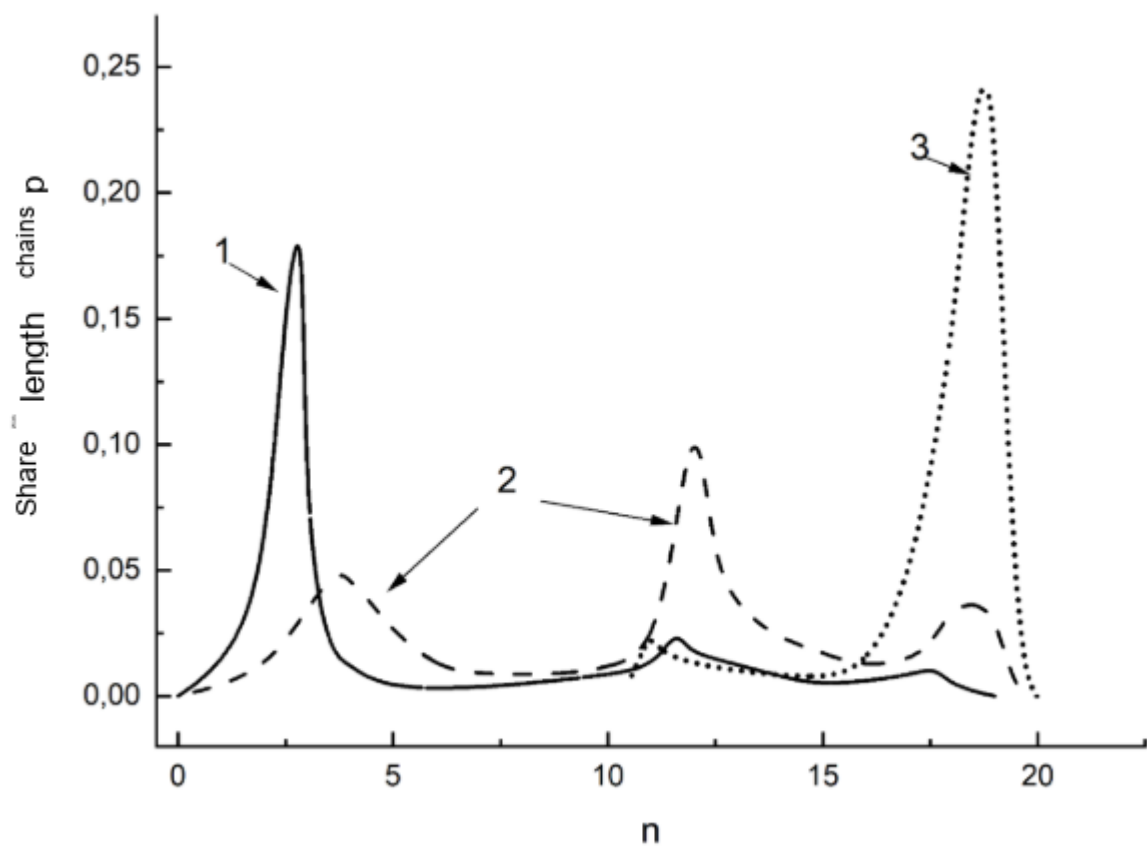
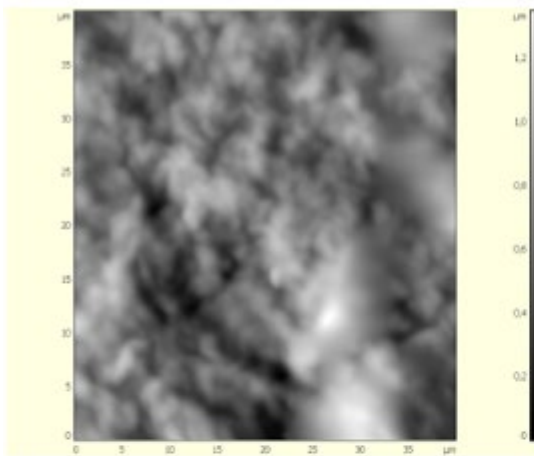
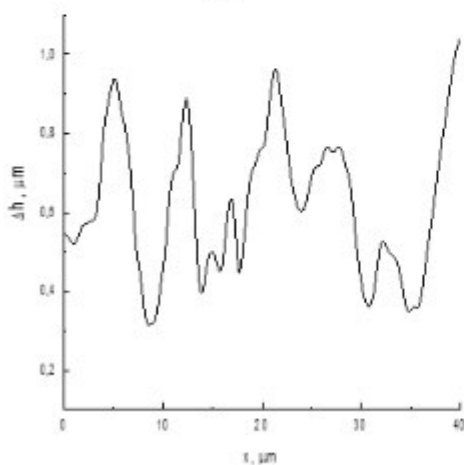


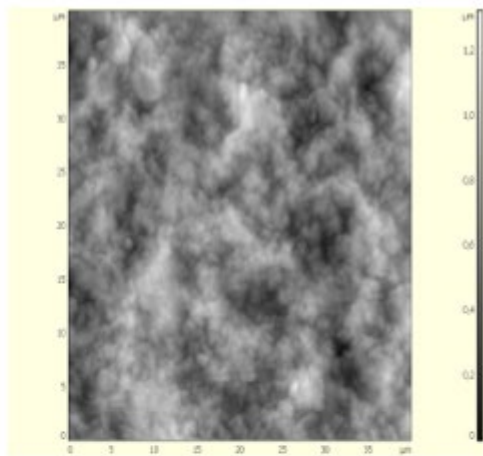
Fig. 1.



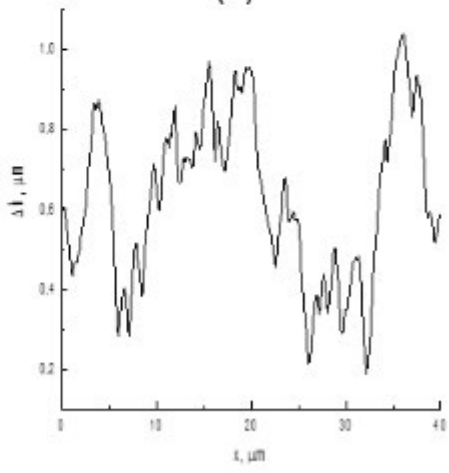
(a)



(a)

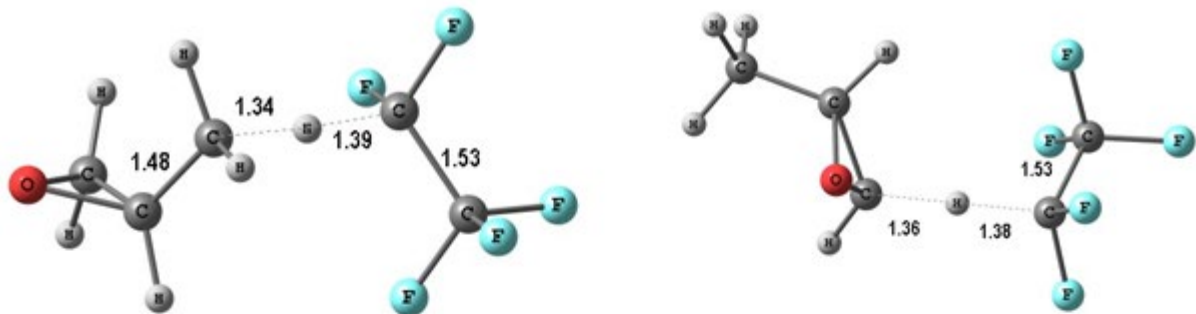


(b)

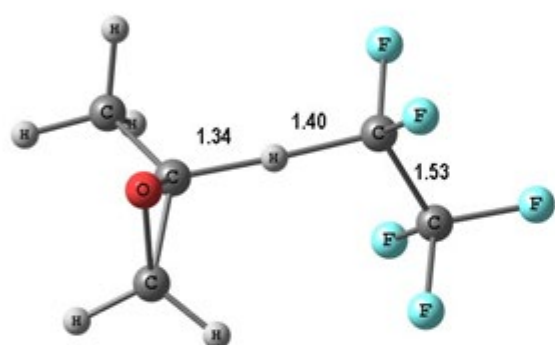


(b)

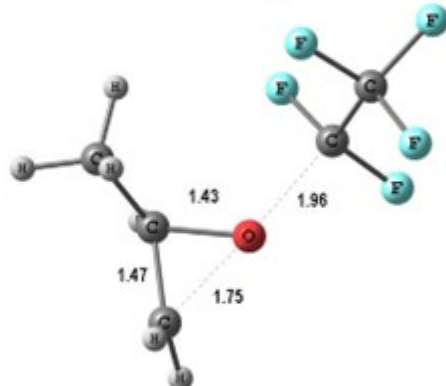
Fig. 2.



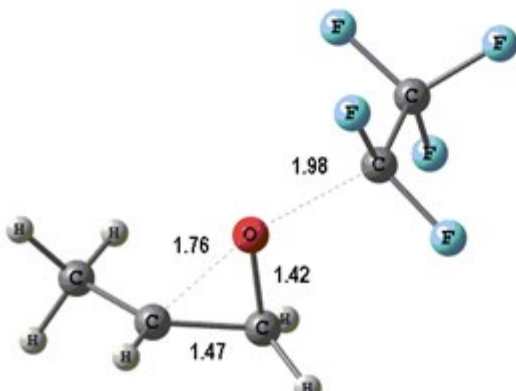
(a)



(b)



(c)



(d)

(e)

Fig. 3.

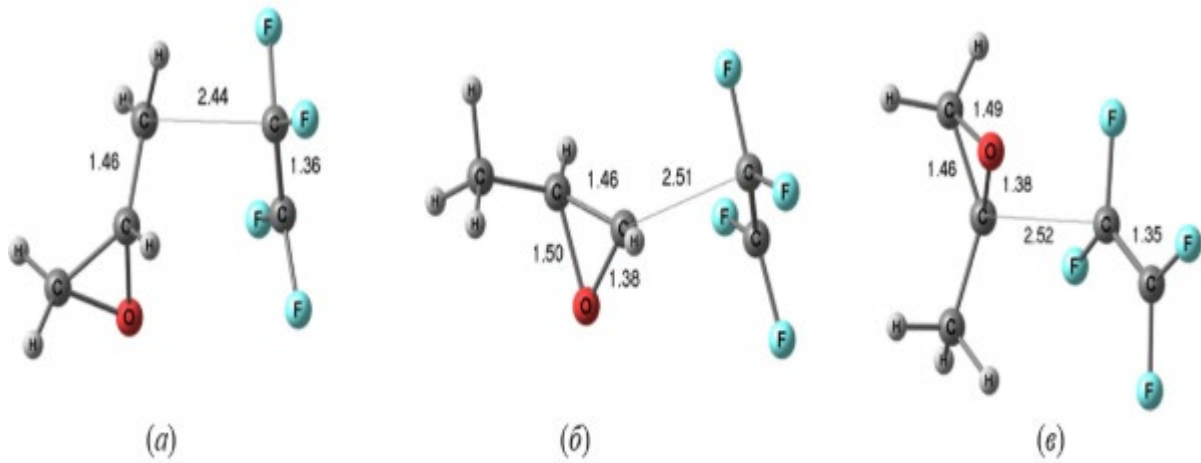


Fig. 4.

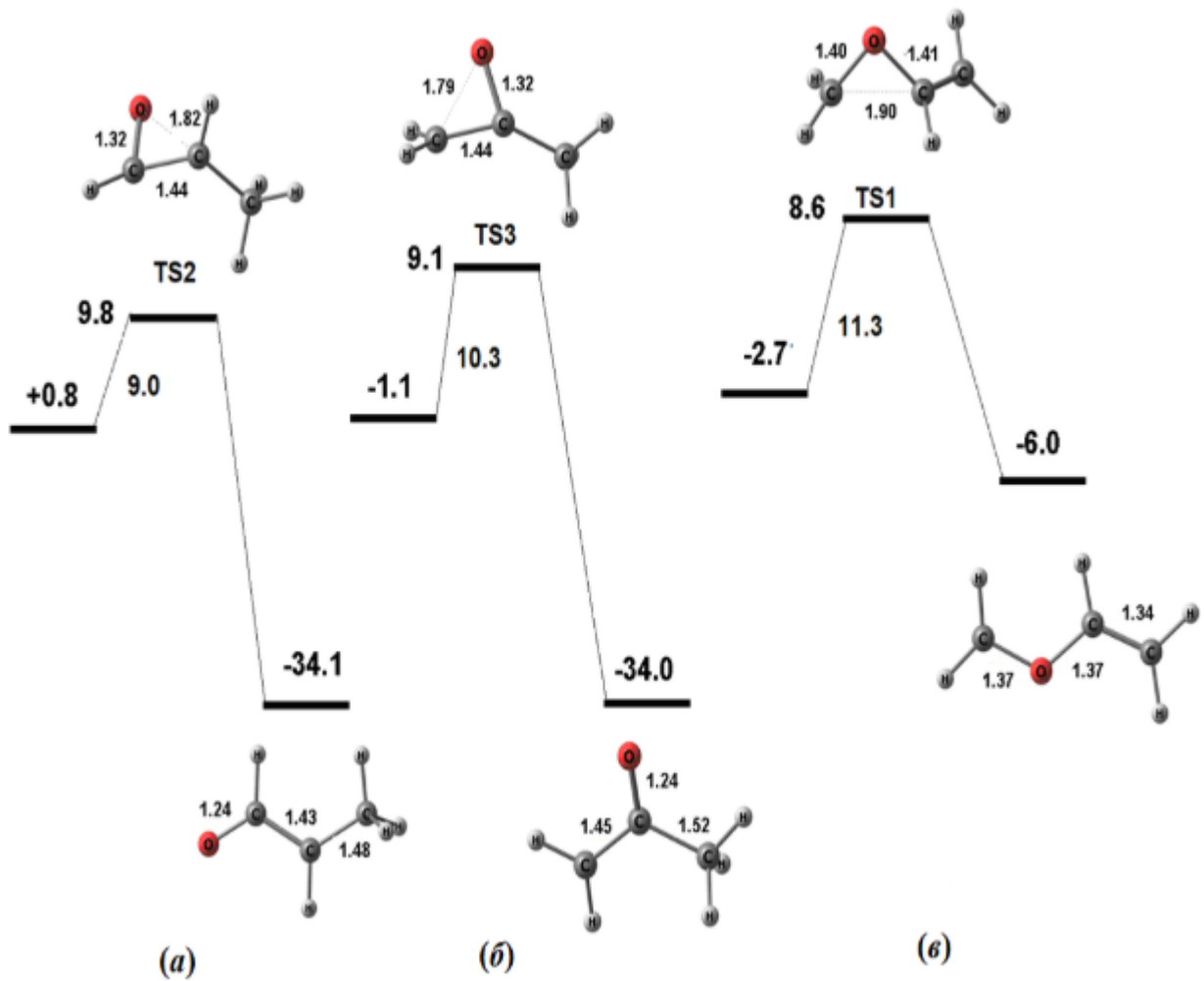


Fig. 5.

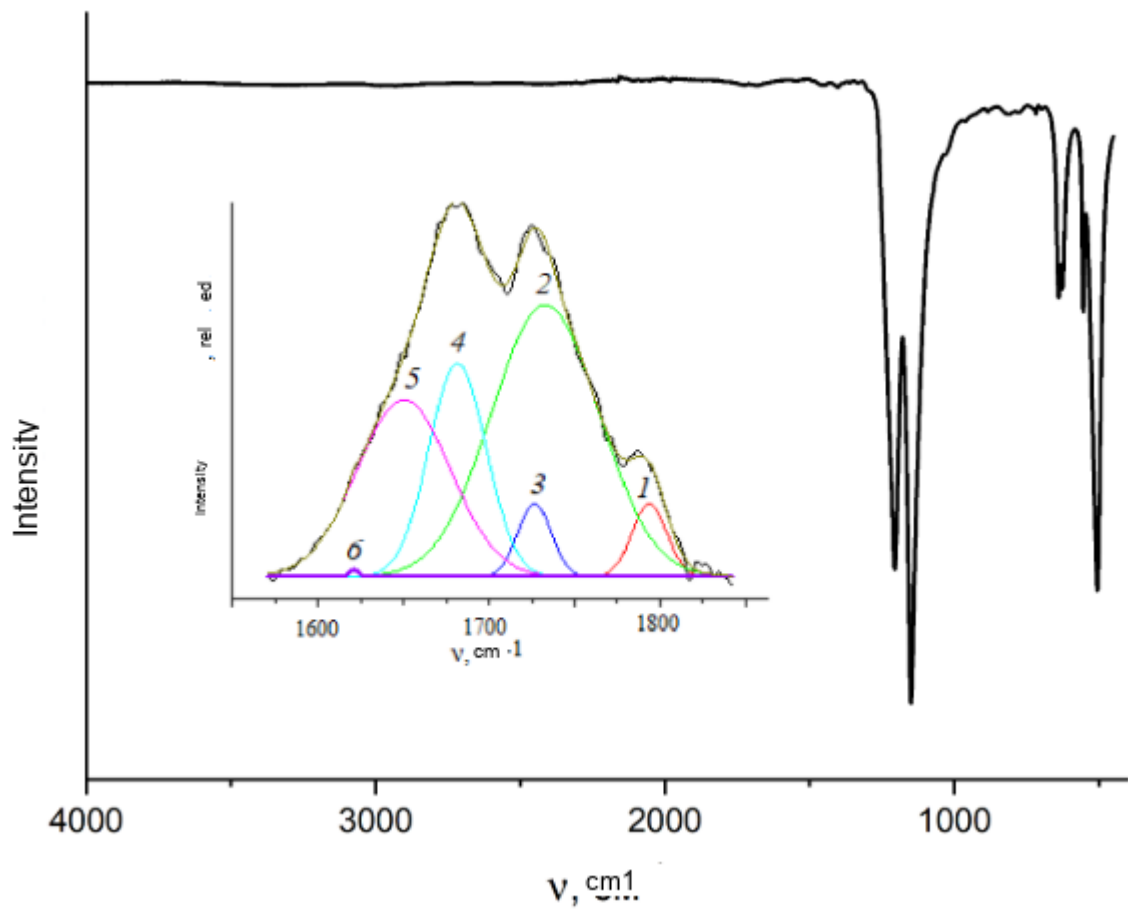


Fig. 6.

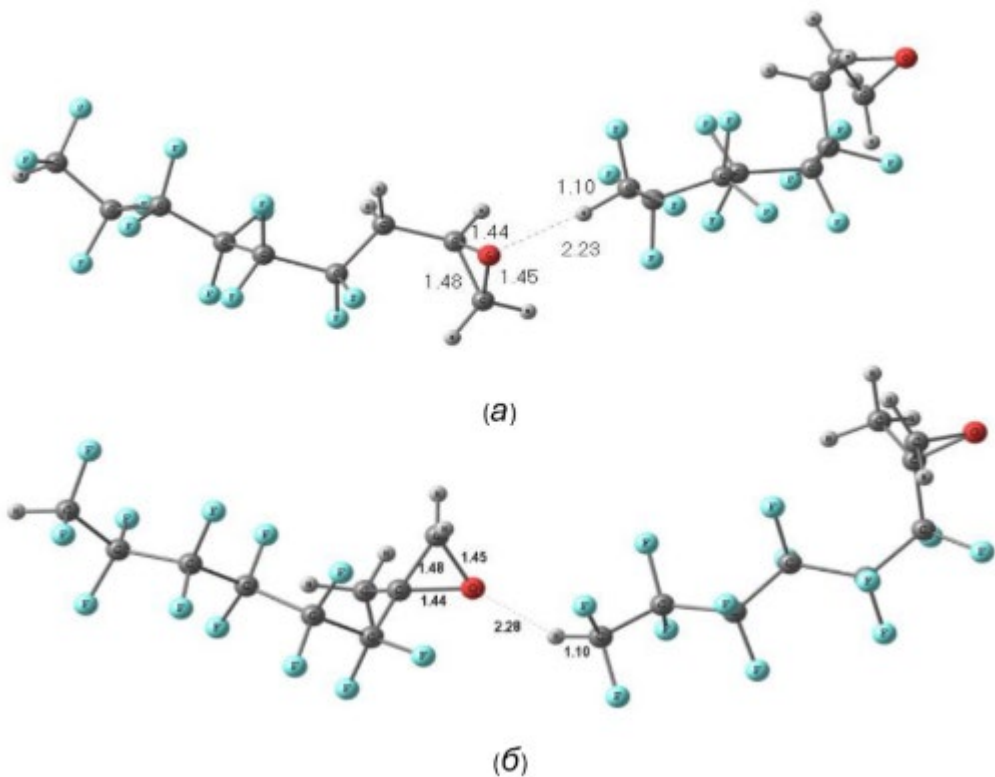


Fig. 7.